Contributed Papers from Materials Science and Technology 2016 (MS&T16)
October 23 – 27, 2016, Salt Palace Convention Center, Salt Lake City, Utah USA

INFLUENCE OF COMPOSITION AND PROCESSING ON THE STRENGTH AND TORSIONAL DUCTILITY OF HIGH STRENGTH STEEL WIRE

C.M. Ciganik[1], J.G. Speer[1], K.O. Findley[1], and W. Van Raemdonck[2]

[1]Advanced Steel Processing and Products Research Center, Colorado School of Mines, Golden, Colorado, USA 80401
[2]N.V. Bekaert S.A., Zwevegem, Belgium

Keywords: high carbon pearlitic steel wire, delamination, mechanical properties

Abstract

High carbon, high strength steel wires are commonly used in applications such as bridge cable, mooring cable, hoisting rope, *etc*. where high tensile strengths and good ductility are desirable parameters. If the wire ductility is insufficient, wires can split longitudinally along the wire axis during torsional loading, also known as delamination. The occurrence and possible origins of delamination have been extensively researched, but no single mechanism has been identified as the primary cause of its initiation. The purpose of this study was to explore relationships between microstructures, tensile properties, and the propensity to delaminate during torsion. Wires were produced with varying carbon and silicon concentrations, and processing variations included Stelmor cooling, intermediate lead patenting, and post-drawing hot-dip galvanizing. As reported previously, the galvanizing treatment induces delamination while the as-drawn wires did not exhibit delamination. Silicon and carbon additions employed for strengthening resulted in a reduced torsional ductility compared to the base alloy. Relationships between tensile and torsional properties indicated that tensile strength is strongly correlated with surface shear stress at delamination. Surface shear strain at delamination was dependent not only on the wire tensile strength, but also on the wire processing history.

Introduction

High carbon pearlitic drawn wire can have strength levels similar to or exceeding those of quenched steels [1]. While strength is critical for many applications, uniform elongation is also essential for good downstream processability, along with torsional ductility. Pearlitic wire must exhibit certain characteristics to achieve these high strengths including fine interlamellar spacing, solid solution strengthening of the ferrite phase, high potential for work hardening, and the ability to maintain its pearlitic microstructure during processing [2, 3].

To increase wire strength, carbon is added to increase the volume fraction of cementite as well as increase the work hardening rate of the steel [2]. It is critical to control transformation behavior at such high levels of carbon in order to avoid the development of grain boundary cementite, which is detrimental to the wire's drawability. Silicon increases strength through solid solution strengthening of ferrite, and is often added to the steel to combat the propensity for the microstructure to spheroidize at elevated processing temperatures such as those experienced during hot-dip galvanizing; the low solubility of silicon in cementite requires it to segregate to the cementite-ferrite interfaces, slowing the diffusion of carbon when heated [3, 4].

In order to generate the fine, pearlitic microstructure desired in industry, Stelmor cooling and lead patenting processes are employed during wire rod and wire production. Lead patenting is the standard heat treatment used in the wire industry and can be done either on wire rod before

drawing, or as an intermediate heat treatment between wire drawing steps. In this process, wire rod is heated into the austenite phase and then isothermally held in an optimal temperature range until the transformation to fine pearlite is completed [5]. During Stelmor cooling, the rod is initially water-cooled from its hot rolling temperature and subsequently formed into rings to be air-cooled on a continuously moving bed to produce a fine pearlitic microstructure [5].

As the strength of the wire is increased, ductility often deteriorates and delamination failure can occur during torsional loading [6]. Delamination is defined as a longitudinal fracture along the wire axis associated with an abrupt drop in torque during twisting [7–9]. Parameters that possibly influence delamination include pearlite colony texture, interlamellar spacing (ILS), the degree of cementite dissolution, the presence of inclusions, residual stresses, and dislocation density caused by plastic deformation during wire drawing [8, 10–12]. Additionally, many studies have reported that wires with higher strength levels are more likely to delaminate [7-9, 13].

This study is a continuation of work by Pennington *et al.* [14] in which steels of varying silicon and carbon levels and varying strengths were chosen to evaluate the effect of wire-strengthening alloying additions on the torsional and post-drawing aging behaviors of high strength steel wire. In this work, an additional higher-carbon alloy is compared to steels similar to the compositions evaluated by Pennington *et al.*, and the effects of processing path during wire drawing and post-drawing galvanizing treatments are evaluated. Finally, relationships between torsional and tensile properties are examined closely as part of a larger study to understand delamination and aging effects.

Experimental Procedure

The materials selected were intended to analyze the effect of carbon and silicon alloying on the mechanical properties of drawn eutectoid wire. Steel compositions of the processed pearlitic wires are given in Table I and include an alloy with low silicon (0.92 wt % C, 0.2 wt % Si), an alloy with high silicon (0.92 wt % C, 1.2 wt % Si), and an alloy with higher carbon and low silicon (1.0 wt % C, 0.2 wt % Si).

Table I. Chemical Compositions of High Strength Steel Wires

wt pct	C	Mn	Si	Ni	Cr	Mo	Al	N	S	P	Cu
0.92 C-0.2 Si	0.93	0.33	0.22	0.016	0.23	0.005	0.001	0.005	0.004	0.006	0.014
1.0 C-0.2 Si	1.01	0.33	0.22	0.016	0.23	0.004	0.001	0.003	0.004	0.008	0.011
0.92 C-1.2 Si	0.94	0.32	1.24	0.013	0.23	0.004	0.001	0.004	0.004	0.005	0.012

During wire production, the wire rods underwent a series of drawing steps to achieve the final wire diameter and surface finish. Initially, wire rods of the three compositions were industrially drawn to two diameters: 13 mm and 12.5 mm. From the starting diameters, half of the material was directly drawn to the final wire diameter (5.3 mm) and half underwent a predrawing step (to 12.5 mm) prior to industrial lead patenting. The predrawn wire rods were patented and subsequently drawn to the final diameter. The drawing reduction for Stelmor cooled wires was approximately 83 % for an initial diameter of 13 mm and 82 % for an initial diameter of 12.5 mm; all lead patented wires experienced an 82 % reduction after patenting. Finally, for both the Stelmor cooled and lead patented wires of all compositions, half of the drawn wire for

each processing condition was industrially hot-dip galvanized while the other half was left uncoated. Hot-dip galvanizing is typically performed at a temperature of about 450 ˚C for approximately 10 seconds.

Tensile testing of as-received wire was conducted on an MTS Alliance RT/100 screw-driven test frame using v-grip wedges designed exclusively for round samples. A crosshead velocity of 2.12 x 10^{-2} mm/s (8.33 x 10^{-4} in/s) was used for testing, resulting in an engineering strain rate of 4.17 x 10^{-4} s^{-1}. Additionally, a 5.08 cm (2 in) Shepic extensometer was employed to measure strain. Three replicate specimens of each condition were tested. Galvanized wires were treated with hydrochloric acid to remove the softer zinc coating in order to prevent slippage and to achieve breakage in the gage length. The hydrochloric acid treatment was conducting by dipping the wire into the hydrochloric acid until the visible reaction was complete and the zinc was removed from the wire; care was taken to prevent a temperature rise in the acid due to the exothermic reaction and wires were cleaned with ethanol after the treatment.

Torsion testing of the wires was conducted on an Instru-Met test frame modified for torsion. Testing was performed at a constant rotational speed of 0.5 revolutions per minute; this low speed ensures that heat generated during testing is sufficiently dissipated to avoid changes in the microstructure. The distance between gripped ends was 13.4 mm (5.25 in) for all samples and three specimens for each condition were tested. The procedure developed by Nadai was employed to calculate the surface shear stress at the moment of delamination [15].

Table II gives the abbreviations used to refer to each condition; an example of this nomenclature would be LC-LSi-S-AD, referring to a low carbon, low silicon alloy, Stelmor cooled, as-drawn sample.

Table II. Nomenclature Used to Identify Steels and Wire Conditions

Term	Abbreviation	Term	Abbreviation
Low Carbon (0.92 wt pct)	LC	Stelmor Cooled	S
High Carbon (1.0 wt pct)	HC	Lead Patented	P
Low Silicon (0.2 wt pct)	LSi	As-Drawn	AD
High Silicon (1.2 wt pct)	HSi	Galvanized	G

Results and Discussion

The averages of selected mechanical properties obtained from the tensile stress-strain curves and torsion torque-twist curves for as-drawn and galvanized wire conditions are summarized in Table III and Table IV, respectively. Tensile properties are specified to meet application requirements; with respect to torsion properties, the surface shear stress and surface shear strain at the moment of delamination were of greatest interest for this study. These two values are used to evaluate the relationship between tensile and torsional properties of the wires.

In order to illustrate the characteristic differences in deformation behavior of the different wire conditions, representative tensile and torsion curves are provided in Figure 1 and Figure 2, respectively. Results for one as-drawn and one galvanized wire for the LC-LSi-P condition are displayed in each figure.

When comparing the overall shape of the tensile curves for the as-drawn and galvanized wires, substantial differences are noted. As a result of end-galvanizing the wires, all wire conditions experienced an increase in yield strength and a substantial increase in uniform elongation, while the work hardening rates at small strains were reduced. Additionally, the

as-drawn wires exhibited a more “roundhouse” yielding behavior whereas the galvanized wires had a more defined yield point.

Table III. Average Tensile and Torsion Properties of As-Drawn Wires*

Sample Condition	Yield Strength (MPa)	Ultimate Tensile Strength (MPa)	Uniform Elongation (pct)	Surface Shear Stress at Delamination (MPa)	Surface Shear Strain at Delamination
LC-LSi-S-AD	1500 ± 38	1860 ± 3	1.48 ± 0.02	-	-
LC-LSi-P-AD	1670 ± 42	2060 ± 1	1.34 ± 0.02	-	-
HC-LSi-S-AD	1620 ± 5	1980 ± 3	1.44 ± 0.01	-	-
HC-LSi-P-AD	1740 ± 32	2190 ± 3	1.37 ± 0.03	-	-
LC-HSi-S-AD	1580 ± 10	2000 ± 10	1.54 ± 0.04	-	-
LC-HSi-P-AD	1860 ± 13	2180 ± 1	1.24 ± 0.01	-	-

*Uncertainty given as ± one standard deviation
- Indicates wire did not delaminate

Table IV. Average Tensile and Torsion Properties of Galvanized Wires*

Sample Condition	Yield Strength (MPa)	Ultimate Tensile Strength (MPa)	Uniform Elongation (pct)	Surface Shear Stress at Delamination (MPa)	Surface Shear Strain at Delamination
LC-LSi-S-G	1600 ± 18	1940 ± 10	4.65 ± 0.21	911 ± 10	0.0746 ± 0.0050
LC-LSi-P-G	1720 ± 5	2060 ± 1	5.40 ± 0.14	1010 ± 1	0.130 ± 0.0040
HC-LSi-S-G	1660 ± 5	2040 ± 7	4.61 ± 0.15	945 ± 16	0.0632 ± 0.0138
HC-LSi-P-G	1810 ± 7	2180 ± 1	5.34 ± 0.14	1050 ± 7	0.0878 ± 0.0059
LC-HSi-S-G	1800 ± 18	2100 ± 9	4.72 ± 0.13	993 ± 7	0.0545 ± 0.0037
LC-HSi-P-G	1950 ± 5	2210 ± 1	5.22 ± 0.03	1100 ± 7	0.0670 ± 0.0093

*Uncertainty given as ± one standard deviation

For all wire compositions, the Stelmor cooled wires exhibited lower ultimate tensile strength than patented wires of the same composition, despite the reduced amount of final cold reduction in the patented condition. Wires that were processed by Stelmor cooling and cold-drawing all experienced an increase in tensile strength after galvanizing.

The change in tensile strength caused by galvanizing of the patented wires was dependent on the wire composition, where the LC-LSi wire showed no strength change, the HC-LSi wire strength was reduced slightly, and the LC-HSi wire strength increased. When a wire undergoes a post-drawing heat treatment, strength is expected to increase initially and subsequently decrease with longer times as cementite decomposition and dislocation recovery occur [8]. In the case of the wire conditions tested, it is interpreted that the LC-LSi and HC-LSi wires have passed the peak strength, whereas the LC-HSi wire has perhaps not yet experienced strength loss due to the galvanizing heat treatment. This result is consistent with previously reported results in which silicon slows the aging process and reduces strength loss from hot-dip galvanizing [1, 5].

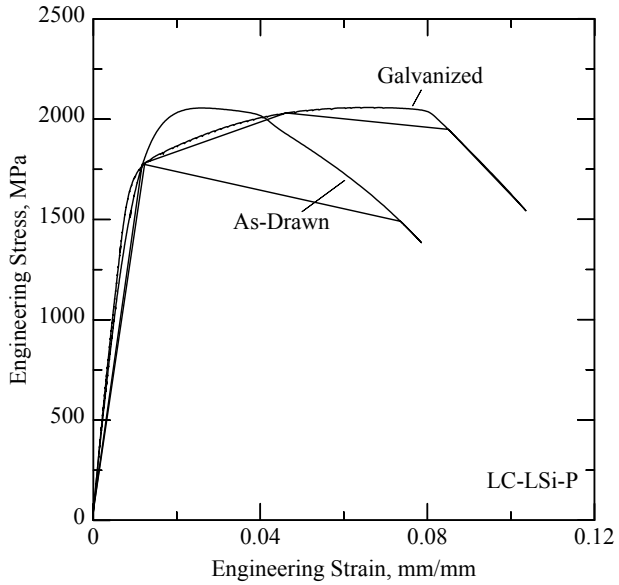

Figure 1. Representative engineering stress-strain curves of two low carbon, low silicon, lead patented wires: one in the as-drawn condition and one in the galvanized condition.

During torsion testing, all of the as-drawn wires failed in a ductile manner and all galvanized wires failed through delamination, resulting in two distinct torque-twist characteristic curve shapes shown in Figure 2. Galvanized wires exhibited higher shear yield strengths than the as-drawn conditions and all patented wires were higher in shear strength than those processed through Stelmor cooling; both of these trends were also found in tension. As expected, delamination failure caused the torsional ductility to be significantly lower for all of the galvanized wires when compared to the as-drawn wires, in contrast to the tensile ductility results where galvanized wire had greater elongations compared to the as-drawn condition.

The addition of either carbon or silicon to the base composition resulted in an increase in surface shear stress at delamination and a reduction in surface shear strain at delamination. Additionally, the LC-HSi wires delaminated immediately after yielding occurred while the HC-LSi wires experienced stress saturation after yielding and prior to delamination. Finally, when comparing the patented wire delamination behavior to that of Stelmor cooled wires, the patented wires not only delaminated at a higher shear stress than the Stelmor cooled wires but delamination failure also occurred at a higher shear strain. From these results it can be suggested that increasing strength does not necessarily correlate to poor torsional ductility.

It is of great interest to better understand how wire tensile properties are related to performance under torsional loading, particularly when delamination occurs. Figure 3 shows the relationships between ultimate tensile strength and two parameters considered fundamentally relevant to fracture in torsion: (a) surface shear stress at delamination and (b) surface shear strain at delamination. This figure only includes galvanized wire conditions as they were the only wires to delaminate during torsion testing. The shear stress at delamination was strongly dependent on the ultimate tensile strength of the wire, and this correlation held for all alloys and processing conditions.

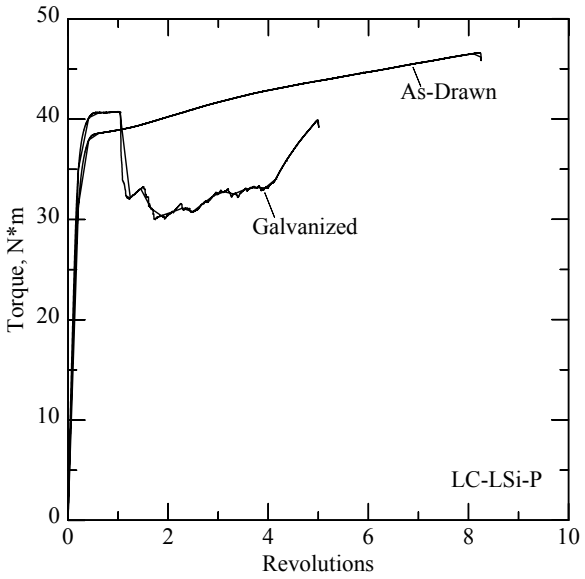

Figure 2. Representative torque-twist curves of two low carbon, low silicon, lead patented wires: one in the as-drawn condition and one in the galvanized condition.

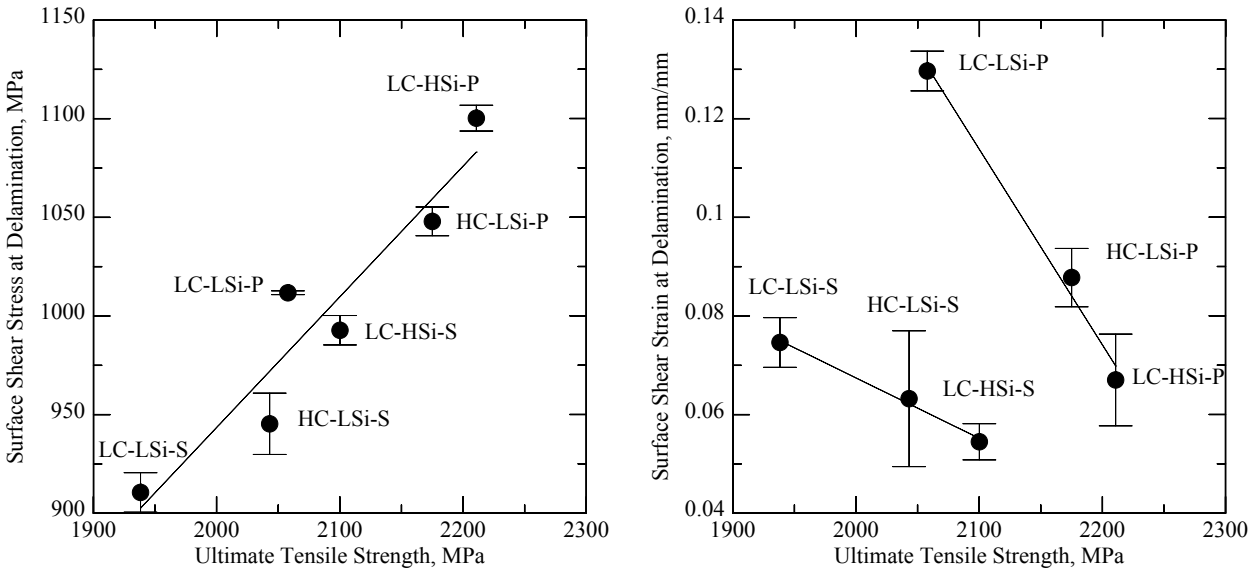

(a) (b)

Figure 3. Ultimate tensile strength correlated with two torsion properties: (a) surface shear stress at delamination and (b) surface shear strain at delamination.

The surface strain at delamination versus ultimate tensile strength is separated by processing condition in Figure 3(b). The shear strain at delamination for the Stelmor cooled wires was less sensitive to a change in ultimate tensile strength than for patented wires. From this result, it is evident that not only is the surface shear strain at delamination dependent on tensile strength, but it is also dependent on the processing conditions and resultant microstructure. Additionally, higher delamination surface shear strains were achieved as a function of tensile

strength when the wire processing included lead patenting rather than direct drawing from Stelmor cooling. It is well known that delamination is affected by pearlite interlamellar spacing (ILS) where a finer ILS corresponds to a reduced propensity for delamination; the more refined microstructure of lead patented wires when compared to Stelmor cooled is thus expected to contribute to the observed trend. It should be noted again that the wire drawing reduction was greater in the Stelmor cooled condition than the drawing reduction after patenting.

Summary

Torsion and tension tests were conducted to elucidate the effects of silicon and carbon additions, processing variations, and post-drawing hot-dip galvanizing on the mechanical properties of high strength pearlitic steel wire. Galvanizing induced wire delamination and reduced torsional ductility despite an increase in tensile ductility when compared to the as-drawn condition, confirming the results of previous studies on the effects of elevated temperature aging on torsional properties. As expected from their more refined microstructure, patented wires not only exhibited higher strengths than the corresponding Stelmor cooled conditions, but also delayed delamination to higher strains under torsional loading. While the high carbon addition increased wire as-drawn strength as desired, a reduced strength after galvanizing and reduced torsional ductility were experienced when compared to the base alloy. The increased silicon addition increased the wire strength after galvanizing by inhibiting cementite decomposition caused by aging at high temperatures, but also reduced the torsional ductility.

When tensile and torsional properties were compared, a strong linear relationship was found between the surface shear stress at delamination and the ultimate tensile strength; therefore, tensile strength was a good indicator of the shear strength at which a wire delaminates, regardless of carbon or silicon alloying variations. Two distinct linear relationships were found to develop for Stelmor and lead patented wire conditions, respectively, when surface shear strain at delamination was related to the ultimate tensile strength. The relationships indicate that better property combinations are achievable with patenting and that microstructure details, in addition to tensile strength, contribute to the propensity for delamination. It was also evident that with increasing tensile strength, the torsional ductility decreased to a greater extent for wires processed through lead patenting versus Stelmor cooling.

Acknowledgements

The authors gratefully acknowledge the support of the sponsors of the Advanced Steel Processing and Products Research Center, an industry-university cooperative research center at the Colorado School of Mines and NV Bekaert for providing the wire for this study.

References

1. T. Tarui, J. Takahashi, H. Tashiro, N. Maruyama, and S. Nishida, “Microstructure control and strengthening of high-carbon steel wires,” *Nippon Steel Tech. Report*, no. 91, pp. 56-61, 2005.

2. H. Tashiro and T. Tarui, “State of the art for high tensile strength steel cord,” *Nippon Steel Tech. Report*, no. 88, pp. 87-91, 2003.

3. Y. Yamaoka, K. Hamada, H. Tsubono, H. Kawakami, Y. Oki, and Y. Kawaguchi, “Development of galvanized high-strength high-carbon steel wire,” *The Iron and Steel Institute of Japan*, vol. 26, pp. 1059-1064, 1986.

4. Y. J. Li, P. Choi, S. Goto, C. Borchers, D. Raabe, and R. Kirchheim, “Evolution of strength and microstructure during annealing of heavily cold-drawn 6.3 GPa hypereutectoid pearlitic steel wire,” *Acta Materialia*, vol. 60, pp. 4005-4016, 2012.

5. G. Krauss, “High-carbon steels: Fully pearlitic microstructures and applications,” in *Steels: Processing, Structure, and Performance*, ASM International, 2005, pp. 281-295.

6. D. B. Park, E. G. Kang, and W. J. Nam, “The prediction of the occurrence of the delamination in cold drawn hyper-eutectoid steel wires,” *Journal of Materials Processing Technology*, vol. 187-188, pp. 178-181, 2007.

7. X. Hu, L. Wang, F. Fang, Z. Ma, Z. H. Xie, and J. Jiang, “Origin and mechanism of torsion fracture in cold-drawn pearlitic steel wires,” *Journal of Materials Science*, vol. 48, pp. 5528-5535, 2013.

8. Z. J. Wang, X. L. Wu, and Y. S. Hong, “Torsion fracture behavior of drawn pearlitic steel wires with different heat treatments,” *Advanced Materials Research*, vol. 33-37, pp. 41-46, 2008.

9. W. Van Raemdonck, I. Lefever, and U. D’Haene, “Torsion tests as a tool for high strength wire evaluation,” *Wire Journal International*, no. 6, pp. 68-75, 1994.

10. W. J. Nam and C. M. Bae, “Void initiation and microstructural changes during wire drawing of pearlitic steels,” *Materials Science and Engineering: A*, vol. 203, pp. 278-285, 1995.

11. J. M. Atienza, J. Ruiz-Hervias, M. L. Martinez-Perez, F. J. Mompean, M. Garcia-Hernandez, and M. Elices, “Residual stresses in cold drawn pearlitic rods,” *Scripta Materialia*, vol. 52, pp. 1223-1228, 2005.

12. M. Zelin and R. M. Shemenski, “Ductility of pearlitic wires under different loading,” *Wire Journal International*, vol. 40, no. 8, pp. 69-73, 2007.

13. W. J. Nam, C. M. Bae, S. J. Oh, and S. J. Kwon, “Effect of interlamellar spacing on cementite dissolution during wire drawing of pearlitic steel wires,” *Scripta Materialia*, vol. 42, pp. 457-463, 2000.

14. R.E. Pennington, W. Van Raemdonck, D.K. Matlock, and G. Krauss, “The Effect of Silicon and Aging on Mechanical Properties and Fracture Response of Drawn High-Strength Pearlitic Steel Wire,” *Wire Journal International*, vol. 44, no. 9, pp. 60-69, 2011.

15. A. Nadai, *Theory of Flow and Fracture of Solids*, 2d ed. New York: McGraw-Hill Book Company, 1950.